

This article was downloaded by:

On: 23 January 2011

Access details: *Access Details: Free Access*

Publisher *Taylor & Francis*

Informa Ltd Registered in England and Wales Registered Number: 1072954 Registered office: Mortimer House, 37-41 Mortimer Street, London W1T 3JH, UK



Journal of Coordination Chemistry

Publication details, including instructions for authors and subscription information:

<http://www.informaworld.com/smpp/title~content=t713455674>

Syntheses, structures and properties of two complexes bridged by $[M(CN)_2]^{2-}$ ($M = Ag(I), Au(I)$)

Mei-Ling Liu^a; Li-Zhi Zhang^a; Xiu-Ping Sun^a; Zhen-Ping Ma^a; Wen Gu^a; Xin Liu^a

^a Department of Chemistry, Nankai University, Tianjin 300071, P.R. China

To cite this Article Liu, Mei-Ling , Zhang, Li-Zhi , Sun, Xiu-Ping , Ma, Zhen-Ping , Gu, Wen and Liu, Xin(2008) 'Syntheses, structures and properties of two complexes bridged by $[M(CN)_2]^{2-}$ ($M = Ag(I), Au(I)$)', Journal of Coordination Chemistry, 61: 14, 2266 – 2273

To link to this Article: DOI: 10.1080/00958970801904802

URL: <http://dx.doi.org/10.1080/00958970801904802>

PLEASE SCROLL DOWN FOR ARTICLE

Full terms and conditions of use: <http://www.informaworld.com/terms-and-conditions-of-access.pdf>

This article may be used for research, teaching and private study purposes. Any substantial or systematic reproduction, re-distribution, re-selling, loan or sub-licensing, systematic supply or distribution in any form to anyone is expressly forbidden.

The publisher does not give any warranty express or implied or make any representation that the contents will be complete or accurate or up to date. The accuracy of any instructions, formulae and drug doses should be independently verified with primary sources. The publisher shall not be liable for any loss, actions, claims, proceedings, demand or costs or damages whatsoever or howsoever caused arising directly or indirectly in connection with or arising out of the use of this material.

Syntheses, structures and properties of two complexes bridged by $[M(CN)_2]^-$ (M = Ag (I), Au (I))

MEI-LING LIU, LI-ZHI ZHANG, XIU-PING SUN,
ZHEN-PING MA, WEN GU and XIN LIU*

Department of Chemistry, Nankai University, Weijin Road, Tianjin 300071, P.R. China

(Received 14 June 2007; in final form 18 October 2007)

A dinuclear complex $Cu_2(bpca)_2(H_2O)_2(Ag_2(CN)_3)$ (**1**) and a 1D complex $[Cu_2(bpca)_2(H_2O)_2(Au(CN)_2)_2]_n$ (**2**) (bpca = bis(2-pyridylcarbonyl)amide anion) have been prepared, structurally characterized and **2** has been magnetically characterized. The magnetic properties show an antiferromagnetic interaction between the two Cu(II) ions. Based on the Hamiltonian $\hat{H} = -2J \sum (S_i \cdot S_{i+1})$, best fitting for the experimental data leads to $J = -0.045 \text{ cm}^{-1}$.

Keywords: Crystal structures; Magnetic properties; Copper(II); Dicyanoaurate; Dicyanoargentate

1. Introduction

Controlled assembly of inorganic coordination polymers from simple building blocks is an important challenge in the design of high-dimensionality systems. In the crystal engineering 'toolbox' [1], hydrogen bonding is perhaps the most used in the design of such supramolecular systems [2], and has been particularly strongly applied towards synthesis of molecular magnetic materials [3–7]. We are currently exploring this concept by studying the supramolecular chemistry of the dicyanoaurate/dicyanoargentate, $[M(CN)_2]^-$ (M = Ag (I), Au (I)), building block, particularly in conjunction with paramagnetic transition-metal cations. Here, we report the syntheses, structures, and spectroscopic properties of two complexes, as well as the magnetic properties of **2**.

2. Results and discussion

2.1. X-ray diffraction studies

A perspective view of **1** is shown in figure 1. The complex, crystallized as $Cu_2(bpca)_2(H_2O)_2(Ag_2(CN)_3)$, belongs to the triclinic system. The Cu(II) ion is a

*Corresponding author. Email: Liuxin64@nankai.edu.cn

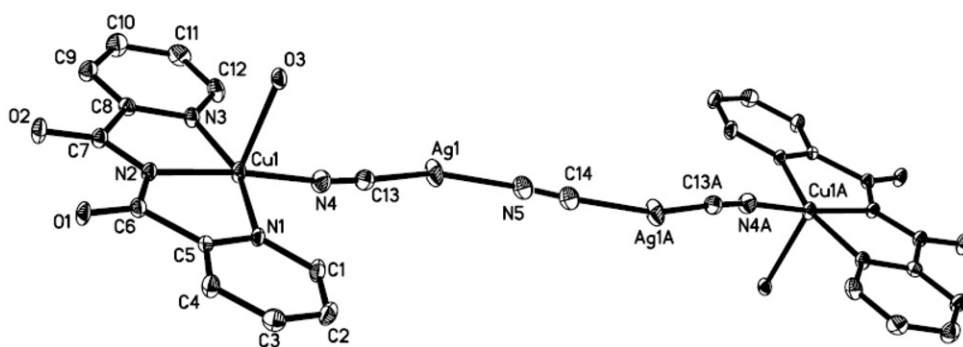


Figure 1. Molecular structure of $[Cu_2(bpca)_2(H_2O)_2(Ag_2(CN)_3)]^-$ (hydrogen atoms omitted for clarity).

distorted square pyramid with the N1, N2, N3, N4 forming the basal plane and O3 occupying the axial position. The deviation of copper is 2.516 Å from the basal plane. Two $[Cu(bpca)]$ units are bridged by $[Ag_2(CN)_3]$ to give a copper to copper separation of 15.022 Å in the centrosymmetric structure. Starting from $[Ag_2(CN)_3]^-$ resulted in condensation polyanions $[Ag_2(CN)_3]^-$ in **1**, leading to a dinuclear structure; performing similar reaction by using $[Au(CN)_2]^-$, complex **2** with 1D extended framework was obtained (figure 2), crystallized as $[Cu_2(bpca)_2(H_2O)_2(Au(CN)_2)_2]_n^-$, also belonging to the triclinic system. Different from the coordination environment of copper in **1**, Cu^{II} of **2** exhibits distorted octahedral geometry with a bpca ligand, a water molecular and two $[Au(CN)_2]^-$ anions. The separation of adjacent copper atoms is 10.085 Å.

2.2. Spectral properties

The room temperature UV-Vis spectra of complex **1** in a DMSO solution, have a weak absorption band at 638 nm (figure 3a), from the $d-d$ transition of $Cu(II)$. Also, UV-Vis spectra give three weak-resolved bands (590, 646, 698 nm) which from a square-pyramidal geometry may correspond to the transitions: ${}^2B_1 \rightarrow {}^2E_g$, ${}^2B_1 \rightarrow {}^2B_2$, ${}^2B_1 \rightarrow {}^2A_1$. Complex **2** also displays a weak absorption band centered at 638 nm (figure 3(b)), from the $d-d$ transition of $Cu(II)$, giving two bands (616, 672 nm) which on a tentatively octahedral geometry may correspond to the transitions: ${}^2B_{1g} \rightarrow {}^2B_2$, ${}^2B_{1g} \rightarrow {}^2A_{1g}$.

EPR experimental and simulation spectra of complexes **1** and **2** at X-band microwave frequencies at room temperature in DMSO are shown in figure 4(a) and 4(b). For **1**, the values of the g tensor can be obtained with $g_x = 2.06$, $g_y = 2.06$, $g_z = 2.18$, which can be used to derive the ground state. In distorted square pyramidal complexes, the unpaired electron occupies the $d_{x^2-y^2}$ orbital with a ${}^2B_{1g}$ ground state resulting in $g_x = g_y = g$ and $g_z = g_{\parallel}$. The observed g values suggest that the unpaired electron lies predominantly in the $d_{x^2-y^2}$ orbital with a distorted square pyramidal environment consistent with the X-ray diffraction analysis. For **2**, the values are $g_x = 2.07$, $g_y = 2.07$, $g_z = 2.22$, $g_x = g_y = g$ and $g_z = g_{\parallel}$, suggesting that the unpaired electron lies predominantly in the $d_{x^2-y^2}$ orbital with an axially elongated octahedral environment consistent with the X-ray diffraction analysis.

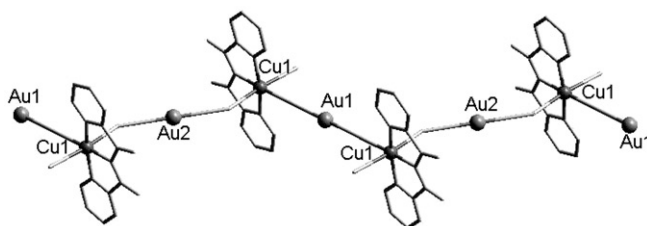


Figure 2. 1D extended framework of $[\text{Cu}_2(\text{bpc})_2(\text{H}_2\text{O})_2(\text{Au}(\text{CN})_2)_2]_n$.

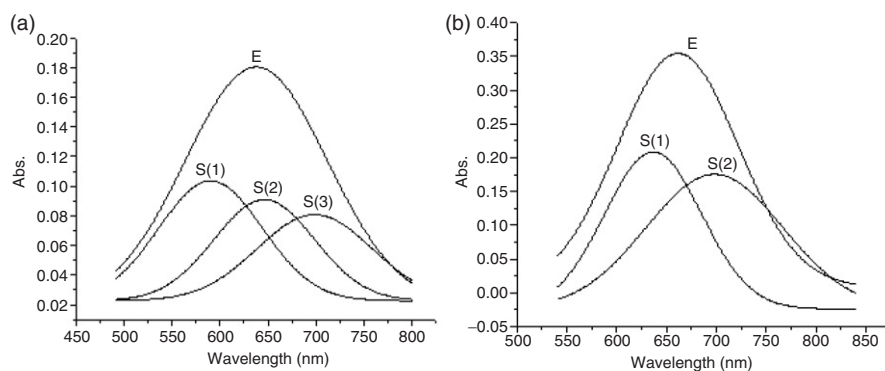


Figure 3. UV-Vis Experimental spectrum (E) and Gauss stimulated spectrum (S) of (a) complex 1; (b) complex 2.

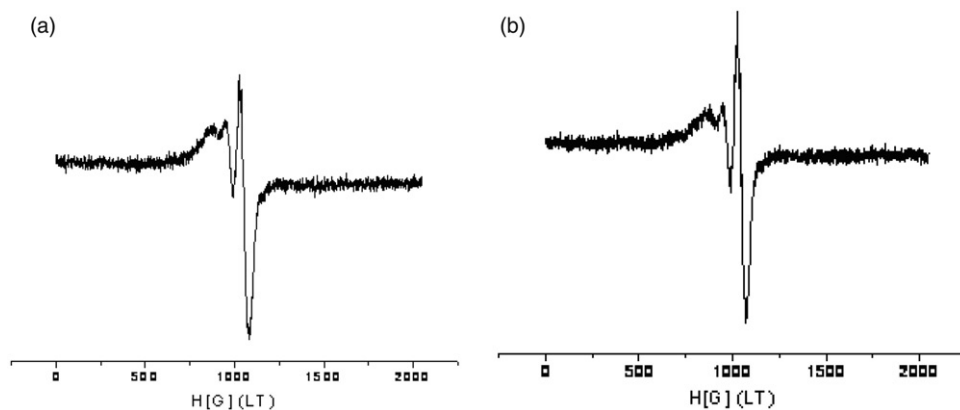


Figure 4. EPR experimental spectra of (a) complex 1; (b) complex 2.

2.3. Magnetic properties

Variable-temperature (2–300 K) magnetic susceptibility data at a magnetic field strength of 2 KG were collected for **2** (figure 5). The μ_{eff} at room temperature, 1.83 B.M., is slightly larger than the spin-only value of 1.73 B.M. for magnetically isolated single-spin Cu^{II} system. When the temperature is lowered, the value of μ_{eff} decreases, indicating that the spins are antiferromagnetically coupled in **2**. From 2 K to 300 K,

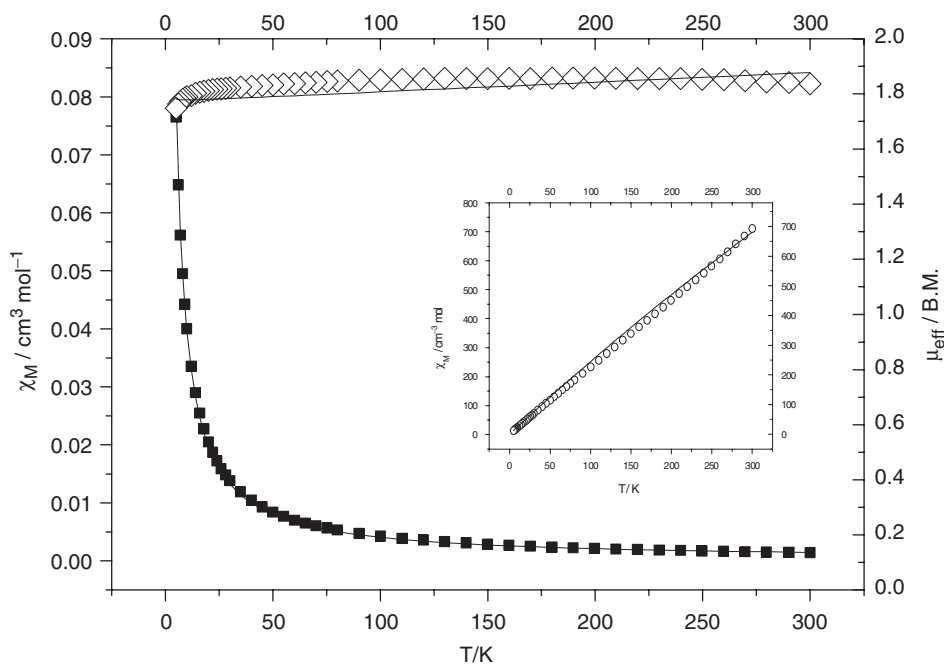


Figure 5. χ_M (■) vs. T and μ_{eff} (□) vs. T plots for **2**. The inset is the $1/\chi_M$ (\hat{b}) vs. T for complex **2**.

the data can be roughly fitted to a Curie–Weiss law with $C = 0.429 \text{ cm}^3 \text{ K mol}^{-1}$ and $\theta = -0.541 \text{ K}$. The Weiss constant is negative which also indicates that the dominant magnetic interaction is antiferromagnetic.

The Hamiltonian for the complex can be written as $\hat{H} = -2J \sum (S_i \cdot S_{i+1})$. Based on the above Hamiltonian, the temperature dependence of the magnetic susceptibility can be expressed as [8]:

$$\chi_M = \frac{Ng^2\beta^2}{kT} \frac{0.25 + 0.074975x + 0.75235x^2}{1.0 + 0.9931x + 0.172134x^2 + 0.75825x^3}$$

$$x = \frac{|J|}{kT}$$

Best fitting for the experimental data leads to $J = -0.045 \text{ cm}^{-1}$, $g = 2.045$ with the agreement factor $R = \sum (\chi_{\text{obsd}} - \chi_{\text{cacld}})^2 / \sum \chi_{\text{obsd}}^2 = 6.4 \times 10^{-4}$. Compared with the reported 1D Cu^{II} complex $\{\text{Cu}(\text{C}_3\text{H}_3\text{NS})_2\text{Cl}_2\}_n$ (Cu–Cu separation of $3.853(4) \text{ \AA}$, $J = -3.81 \text{ cm}^{-1}$)[9], **2** displays weaker antiferromagnetic properties (Cu–Cu separation of 10.005 \AA).

3. Experimental

3.1. Physical measurements

Infrared spectra as a KBr pellet were recorded on a Bruker Tensor 27 spectrophotometer in the range of $4000\text{--}400 \text{ cm}^{-1}$. The UV-Vis spectrum in DMSO was

Table 1. Crystal data and structure refinement for **1** and **2**.

Empirical formula	C ₁₄ H ₁₀ AgCuN ₅ O ₃ (1)	C ₂₈ H ₂₀ Au ₂ Cu ₂ N ₁₀ O ₆ (2)
Formula weight	467.68	1113.55
Temperature (K)	294(2)	293(2)
λ (Mo-K α) (Å)	0.71073	0.71073
Crystal system	Triclinic	Triclinic
Space group	<i>P</i> $\bar{1}$	<i>P</i> $\bar{1}$
Unit cell dimensions (Å, °)		
<i>a</i>	7.254(2)	7.8124(9)
<i>b</i>	10.178(3)	8.5139(11)
<i>c</i>	10.640(3)	12.8593(15)
α	100.489(5)	104.4580(10)
β	95.691(5)	103.5620(10)
γ	95.143(4)	96.755(2)
<i>V</i> (Å ³)	763.9(4)	790.92(17)
<i>Z</i>	2	1
<i>D</i> _{calcd} (Mg m ⁻³)	2.033	2.338
Abs. Coeff. (mm ⁻¹)	2.697	10.631
<i>F</i> (000)	458	522
Crystal size (mm ³)	0.24 × 0.16 × 0.12	0.32 × 0.20 × 0.12
2 θ range (°)	1.96 to 25.01	2.51 to 25.03
Limiting indices	-8 ≤ <i>h</i> ≤ 8 -12 ≤ <i>k</i> ≤ 12 -12 ≤ <i>l</i> ≤ 6	-8 ≤ <i>h</i> ≤ 9 -9 ≤ <i>k</i> ≤ 10 -15 ≤ <i>l</i> ≤ 15
Reflections collected	3772	4341
Unique reflections	2658 (R(int)=0.0239)	2756 [R (int)=0.0156]
Absorption correction	Semi-empirical from equivalents	
Max. and min. transmission	1.000000 and 0.458046	
Refinement method	Full-matrix least-squares on <i>F</i> ²	Full-matrix least-squares on <i>F</i> ²
Data/restraints/parameters	2658/16/226	2756/3/221
Goodness-of-fit on <i>F</i> ²	1.213	1.037
Final <i>R</i> indices (<i>I</i> > 2 σ (<i>I</i>))	<i>R</i> ₁ = 0.0601, <i>wR</i> ₂ = 0.1524	<i>R</i> ₁ = 0.0217, <i>wR</i> ₂ = 0.0527
<i>R</i> indices (all data)	<i>R</i> ₁ = 0.0777, <i>wR</i> ₂ = 0.1612	<i>R</i> ₁ = 0.0273, <i>wR</i> ₂ = 0.0555
Largest diff. Peak hole (e Å ⁻³)	1.071 and -1.104	0.468 and -0.455
Primary method of solution	Direct	Direct
Computing data collection	Bruker SMART	Bruker SMART
Computing cell refinement	Bruker SMART	Bruker SMART
Computing structure solution	SHELXL-97	SHELXS-97
Computing structure refinement	SHELXL-97	SHELXL-97

recorded on a Jasco V-570 UV-Vis scanning spectrophotometer. The ESR spectrum was recorded on an ER 200D-SRC ESR spectrophotometer.

3.2. Starting materials

KAg(CN)₂ and KAu(CN)₂ were of analytical grade and were obtained from commercial sources and used without further purification. [Cu(bpca)(H₂O)(NO₃)] \cong H₂O was synthesized according to the literature[10].

3.3. Synthesis of [Cu₂(bpca)₂(Ag₂(CN)₃)] (**1**) and [Cu₂(bpca)₂(H₂O)₂(Au(CN)₂)₂]_{*n*}

1 was synthesized from the slow diffusion of two aqueous solutions in an H-shaped vessel. One side contained [Cu(bpca)(H₂O)(NO₃)]·H₂O (0.2 mmol, 2 mL); the other

Table 2. Selected bond lengths (\AA) and angles ($^\circ$) for **1** and **2**.

Complex 1	Complex 2
Cu(1)–N(2)	Cu(1)–O(3)
Cu(1)–N(4)	Cu(1)–N(2)
Cu(1)–N(3)	Cu(1)–N(4)
Cu(1)–N(1)	Cu(1)–N(1)
Cu(1)–O(3)	Cu(1)–N(3)
	Cu(1)–N(5)
N(2)–Cu(1)–N(4)	N(2)–Cu(1)–N(4)
N(2)–Cu(1)–N(3)	N(2)–Cu(1)–N(1)
N(4)–Cu(1)–N(3)	N(4)–Cu(1)–N(1)
N(2)–Cu(1)–N(1)	N(2)–Cu(1)–N(3)
N(4)–Cu(1)–N(1)	N(4)–Cu(1)–N(3)
N(3)–Cu(1)–N(1)	N(1)–Cu(1)–N(3)
N(2)–Cu(1)–O(3)	C(1)–N(1)–Cu(1)
N(4)–Cu(1)–O(3)	C(5)–N(1)–Cu(1)
N(3)–Cu(1)–O(3)	C(7)–N(2)–Cu(1)
N(1)–Cu(1)–O(3)	C(6)–N(2)–Cu(1)
Cu(1)–O(3)–	C(12)–N(3)–
H(3A)	Cu(1)
Cu(1)–O(3)–	C(8)–N(3)–Cu(1)
H(3B)	
C(5)–N(1)–Cu(1)	C(13)–N(4)–
	Cu(1)
C(1)–N(1)–Cu(1)	
C(7)–N(2)–Cu(1)	
C(6)–N(2)–Cu(1)	
C(12)–N(3)–	
Cu(1)	
C(8)–N(3)–Cu(1)	
C(13)–N(4)–	
Cu(1)	
1.947(6)	2.653(5)
1.970(7)	1.937(3)
1.994(7)	1.942(3)
2.006(7)	1.992(3)
2.391(7)	1.997(3)
	2.509
172.7(3)	177.49(16)
82.0(3)	82.22(12)
97.2(3)	97.90(13)
81.0(3)	82.14(12)
99.1(3)	97.63(13)
162.2(3)	164.19(12)
93.6(3)	128.2(3)
93.8(3)	113.9(2)
94.1(3)	117.6(2)
92.0(3)	117.4(2)
95.3	127.5(3)
146.8	113.6(2)
114.1(5)	176.4(4)
128.1(6)	
117.5(5)	
118.6(5)	
129.0(6)	
114.0(5)	
170.4(8)	

contained a solution of $\text{K}[\text{Ag}(\text{CN})_2]$ (0.2 mmol, 2 mL). Blue prismatic crystals were formed two weeks later, collected by filtration, washed with a small amount of cold water and dried. The yield is approximately 20% (based on Cu). Anal. Calcd for $\text{C}_{14}\text{H}_{10}\text{AgCuN}_5\text{O}_3$: C, 57.91; H, 3.61; N, 20.60; found: C, 56.76; H, 3.42; N, 23.64. IR (KBr pellet): 3481 (s), 2131 (w), 1702 (s), 1367 (s).

2 was prepared according to the same method as **1** in an H-shaped vessel. One side contained $[\text{Cu}(\text{bpca})(\text{H}_2\text{O})(\text{NO}_3)] \cdot \text{H}_2\text{O}$ (0.2 mmol, 2 mL) and the other contained a solution of $\text{K}[\text{Au}(\text{CN})_2]$ (0.2 mmol, 2 mL). Blue prismatic crystals were formed two weeks later, collected by filtration, washed with a small amount of cold water and dried. The yield is approximately 15% (based on Cu). Anal. Calcd for $\text{C}_{14}\text{H}_{10}\text{AuCuN}_5\text{O}_3$: C, 30.29; H, 1.70; N, 12.49; found: C, 30.20; H, 1.81; N, 12.58%. IR (KBr pellet): 2203 (w), 2149 (w), 1701 (s), 1363 (s).

3.4. X-ray structure analysis

Structural measurements of the two complexes were performed on a computer controlled Bruker SMART 1000 CCD diffractometer equipped with graphite-monochromated Mo- $K\alpha$ radiation with radiation wavelength 0.71073 Å at room temperature by using the ω -scan technique. Lorentz polarization and absorption corrections were applied. The structures were solved by using SHELXL-97 and refined by the full-matrix least-squares method. Non-hydrogen atoms were refined anisotropically. Hydrogen atoms were located from the difference Fourier map and refined. Crystal data and structure refinement for **1** and **2** are shown in table 1 and selected bond lengths and angles are given in table 2.

Supplementary material

Crystallographic data (excluding structure factors) for the structures in this article have been deposited with Cambridge Crystallographic Data Center as supplementary publication CCDC Nos 294551 and 277120. Copies of the data can be obtained free of charge on application to Cambridge Crystallographic Data Center, 12 Union Road, Cambridge CB2 1EZ, UK (Fax: -44-1223-336033; Email for inquiry: fileserv@ccdc.cam.ac.uk; Email for deposition: deposit@ccdc.cam.ac.uk).

Acknowledgements

This work was supported by the National Natural Science Foundation of China (Grant 20371027 and 20071020) and Tianjin Science Foundation (Grant 033609211).

References

- [1] D. Braga, F. Grepioni, G.R. Desiraju. *Chem. Rev.*, **98**, 1375 (1998).
- [2] M.J. Zaworotko. *Chem. Soc. Rev.*, 283 (1994).

- [3] O. Kahn (Ed.). *Magnetism: A Supramolecular Function*, Kluwer, Dordrecht (1996).
- [4] J. Veciana, J. Cirujeda, C. Rovira, E. Molins, J.J. Novoa. *J. Phys. I France*, **6**, 1967 (1996).
- [5] N. Yoshioka, M. Irisawa, Y. Mochizuki, T. Kato, H. Inoue, S. Ohba. *Chem. Lett.*, 251 (1997).
- [6] A. Lang, Y. Pei, L. Ouahab, O. Kahn. *Adv. Mater.*, **8**, 60 (1996).
- [7] M.M. Matsushita, A. Izuoka, T. Sugawara, T. Kobayashi, N. Wada, N. Takeda, M. Ishikawa. *J. Am. Chem. Soc.*, **119**, 4369 (1997).
- [8] M. Mimura, T. Matsuo, T. Nakashima, N. Matsumoto. *Inorg. Chem.*, **37**, 3553 (1998).
- [9] W.E. Estes, D.P. Gavel, W.E. Hathiald, D.J. Hodgeson. *Inorg. Chem.*, **17**, 1415 (1978).
- [10] A. Cantarero, J.M. Amigo, J. Faus, M. Julve, T. Debaeremaker. *J. Chem. Soc., Dalton Trans.*, 2033 (1988).